DOI: 10.6060/ivkkt.20236607.6835j

УДК: 537.528+541.15

ГАЗОВЫЕ РАЗРЯДЫ КАК ИНСТРУМЕНТ ОЧИСТКИ ГАЗОВЫХ И РАСТВОРНЫХ СРЕД И СИНТЕЗА НЕОРГАНИЧЕСКИХ МАТЕРИАЛОВ

А.А. Гущин, В.И. Гриневич, Е.Ю. Квиткова, Г.И. Гусев, Д.А. Шутов, А.Н. Иванов, А.С. Манукян, В.В. Рыбкин

Андрей Андреевич Гущин (ORCID 0000-0003-2655-1671), Владимир Иванович Гриневич (ORCID 0000-0002-9400-703X), Елена Юрьевна Квиткова (ORCID 0000-0003-3366-9483), Григорий Игоревич Гусев (ORCID 0000-0003-3366-9483)

Кафедра промышленной экологии, Ивановский государственный химико-технологический университет, Шереметевский пр., 7, Иваново, 153000, Россия

Дмитрий Александрович Шутов (ORCID 0000-0002-4662-4631), Александр Николаевич Иванов (ORCID 0000-0002-5207-7582), Анна Славиковна Манукян (ORCID 0000-0003-3944-3282), Владимир Владимирович Рыбкин (ORCID 0000-0001-7295-7803)*

Кафедра технологии приборов и материалов электронной техники, Ивановский государственный химико-технологический университет, Шереметевский пр., 7, Иваново, 153000, Россия
E-mail: rybkin@isuct.ru

В статье приводится обзор результатов исследований процессов очистки газовых и растворных сред от органических (тетрахлорметан, 1,4-дихлорбензол и 2,4-дихлорфенол, и др.) и неорганических (Cr(VI), Mn(VII), Cu^{2+}, Fe^{2+3+}, Zn^{2+}, Cd^{2+}, Ni^{2+} и др.) веществ, а также синтеза оксидных материалов на основе вышеуказанных металлов под действием диэлектрического барьерного разряда (ДБР) и разряда постоянного тока атмосферного давления. Работы выполнены в совместных исследованиях, проведенных на кафедрах Промышленной экологии и Технологии приборов и материалов электронной техники ИГХТУ за последние 10 лет. В результате исследований выявлены кинетические закономерности разложения вышеуказанных органических веществ, т.е. определены эффективные константы скорости и скорости реакций разложения и их зависимости от параметров ДБР (мощности, расхода газа и раствора). На основе этих данных найдены энергетические эффективности процессов разложения. Определены основные продукты разложения и их зависимости от параметров разряда. Предложены вероятные механизмы протекающих процессов. Показано, что действие разряда постоянного тока на водные растворы приводит к восстановлению Cr(VI) и Mn(VII) в составе $Cr_2O_7^{2-}$ и MnO_4^- до ионов Cr^{3+} и Mn^{2+}. При действии того же разряда на растворы солей, содержащих ионы Cu^{2+}, Fe^{2+3+}, Zn^{2+}, Cd^{2+}, Ni^{2+}, наблюдается образование коллоидных растворов гидроксосоединений указанных ионов. Методами ДРС, СЭМ, ЭРС, РФА ТГА, ДСК определены размеры получающихся частиц их фазовый и химический состав. Показано, что прокалка полученных частиц приводит к образованию кристаллических оксидов соответствующих металлов. Таким образом, действие разряда обеспечивает очистку водных растворов от тяжелых металлов с образованием оксидных материалов наноразмерного диапазона, которые обладают полупроводниковыми и каталитическими свойствами.

Ключевые слова: газоразрядная плазма, очистка водных растворов, органические и неорганические поллютанты, синтез оксидных материалов

Для цитирования:
Гущин А.А., Гриневич В.И., Квиткова Е.Ю., Гусев Г.И., Шутов Д.А., Иванов А.Н., Манукян А.С., Рыбкин В.В. Газовые разряды как инструмент очистки газовых и растворных сред и синтеза неорганических материалов. *Изв. вузов. Химия и хим. технология*. 2023. Т. 66. Вып. 7. С. 120–131. DOI: 10.6060/ivkkt.20236607.6835j.

For citation:
Guschin A.A., Grinevich V.I., Kvitkova E.Yu., Gusev G.I., Shutov D.A., Ivanov A.N., Manukyan A.S., Rybkin V.V. Gas discharges as a tool for cleaning gas and solution mediums and synthesis of inorganic materials. *ChemChemTech [Izv. Vyssh. Uchebn. Zaved. Khim. Khim. Tekhnol.]*. 2023. V. 66. N 7. P. 120–131. DOI: 10.6060/ivkkt.20236607. 6835j.

GAS DISCHARGES AS A TOOL FOR CLEANING GAS AND SOLUTION MEDIUMS AND SYNTHESIS OF INORGANIC MATERIALS

A.A. Guschin, V.I. Grinevich, E.Yu. Kvitkova, G.I. Gusev, D.A. Shutov, A.N. Ivanov, A.S. Manukyan, V.V. Rybkin

Andrey A. Gushchin (ORCID 0000-0003-2655-1671), Vladimir I. Grinevich (ORCID 0000-0002-9400-703X), Elena Yu. Kvitkova (ORCID 0000-0003-3366-9483), Grigoriy I. Gusev (ORCID 0000-0003-3366-9483)

Department of Industrial Ecology, Ivanovo State University of Chemistry and Technology, Sheremetevskiy ave., 7, Ivanovo, 153000, Russia

Dmitry A. Shutov (ORCID 0000-0002-4662-4631), Alexander N. Ivanov (ORCID 0000-0002-5207-7582), Anna S. Manukyan (ORCID 0000-0003-3944-3282), Vladimir V. Rybkin (ORCID 0000-0001-7295-7803)*

Department of Microelectronic Devices and Materials, Ivanovo State University of Chemistry and Technology, Sheremetevskiy ave., 7, Ivanovo, 153000, Russia
E-mail: rybkin@isuct.ru*

The article provides an overview of the results of research of the purification processes of gas and solution media from organic (tetrachloromethane, 1,4-dichlorobenzene and 2,4-dichlorophenol, etc.) and inorganic (Cr(VI), Mn(VII), Cu^{2+}, Fe^{2+3+}, Zn^{2+}, Cd^{2+}, Ni^{2+}, etc.) substances, as well as the synthesis of oxide materials based on the above metals under the action of a dielectric barrier discharge (DBD) and atmospheric pressure DC discharge. The work was carried out in joint research conducted at the Departments of Industrial Ecology and Microelectronic Devices and Materials of the ISUCT over the past 10 years. As a result of the research, the kinetic regularities of decomposition of the above organic substances were revealed, i.e. the rate and effective rate constants of the decomposition reactions and their dependences on the DBR parameters (power, gas and solution flow rates) were determined. On the basis of these data, the energy efficiency of decomposition processes was found. The main decomposition products and their dependence on the discharge parameters are determined. Probable mechanisms of the ongoing processes were proposed. It is shown that the action of a direct current discharge on aqueous solutions leads to the reduction of Cr(VI) and Mn(VII) in the composition of $Cr_2O_7^{2-}$ and MnO_4^- to Cr^{3+} and Mn^{2+} ions. When the same discharge acts on solutions of salts containing Cu^{2+}, Fe^{2+3+}, Zn^{2+}, Cd^{2+}, Ni^{2+} ions, the formation of colloidal solutions of hydroxo compounds of these ions is observed. The sizes of resulting particles, their phase and chemical composition were determined by DLS, SEM, EDX, TGA, XRD, DSC methods. It is shown that the calcination of the obtained particles leads to the formation of crystalline oxides of the corresponding metals. Thus, the action of the discharge ensures the purification of aqueous solutions from heavy metals with the formation of oxide materials of the nanoscale range, which have semiconductor and catalytic properties.

Key words: gas-discharge plasma, aqueous solutions purification, organic and inorganic pollutants, oxide materials synthesis

INTRODUCTION

In the past 20 years, over 1000 works devoted to the properties of atmospheric-pressure discharges operating above and under the surfaces of water media have been published (see [1-4]). Interest in such discharges is motivated by both the need to gain insight into their physics and chemistry and the possibility of using them to solve a number of practical problems. Among these problems, we can mention biomedical applications [5, 6], excitation sources for atomic emission spectroscopy, modification of the surface properties of polymer materials and immobilization of other molecules on them (e.g., heterocyclic compounds [7, 8]), preparation of catalyst nano powders and semiconducting compounds, synthesis of fullerenes [9], purification of wastewaters and gas exhausts from organic compounds [10], etc. It is also proposed to use discharge systems to remove pesticides from vegetables and to remediate of polluted soils [11, 12]. Plasma systems are attractive because, under their action on water, a vast variety of chemically active particles possessing ether oxidizing or reducing properties are generated. The main oxidizers

are OH radicals (the standard oxidizing potential E^0 = 2.85 V), O atoms (E^0 = 2.42 V), hydrogen peroxide (E^0 = 1.68 V), ozone (E^0 = 1.51 V), and HO_2 (E^0 = 1.70 V), while the main reducing agents are hydrogen atoms (E^0 = –2.3 V) and molecules and solvated electrons (E^0 = –2.68 V). These particles are formed without any additional chemical reagents, while the ambient air can serve as a plasma-forming gas. Also, the action of the discharge on water leads to a change in its pH. Whether water is a cathode or an anode, pH decreases or increases [13].

In this article, we present the results of our research on the decomposition of some organic chlorine-containing compounds both in the gas phase and in aqueous solutions. The results of studies on the purification of aqueous solutions from heavy metals are also presented. At the same time, the resulting chemical compounds make it possible to obtain practically important substances with catalytic, semiconductor and magnetic properties. Moreover, the particle sizes of these substances can lie in the nanometer range.

EXPERIMENTAL SETUP

Two types of DBD reactors were used in the work, the schemes of which are shown in Figs. 1, 2. In all cases, the discharge was excited from a high-voltage power supply of industrial frequency (50 Hz). Set-up in Fig. 1 was used to process gas mixtures. The main plasma-forming gas from cylinder *1* was passed through cell *2*, where it was saturated with pollutant vapor. The resulting mixture of gases entered the DBD *4* cylindrical reactor. The treated gas was collected in vessel *5*, from where it entered the chemical analysis.

A falling film reactor was used to treat aqueous solutions (Fig. 2). The solution in the film mode flowed down over the surface of the inner electrode covered with fiberglass. The treated solution was analyzed chemically.

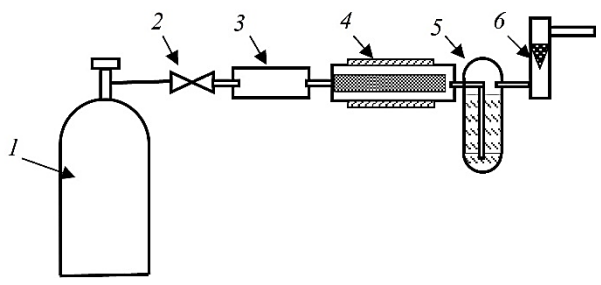

Fig. 1. The scheme of the experimental setup for gas treatment. 1 - oxygen balloon, 2 – valve, 3 - cell with pollutant, 4 – DBD reactor, 5 - absorption vessel, 6 – flow meter

Рис. 1. Схема экспериментальной установки для очистки газа. 1 - кислородный баллон, 2 - вентиль, 3 - ячейка с поллютантом, 4 - реактор ДБД, 5 - абсорбционная емкость, 6 – расходомер

For the treatment of aqueous solutions by a direct current (DC) glow discharge, reactors were used, the designs of which are shown in Fig. 3 and 4. The discharge was ignited by applying a high voltage between the surface of the solution and the outer metal electrode(s). For fig. 3, the solution served as the cathode, and for Fig. 4 one part of the solution was the cathode and the other the anode.

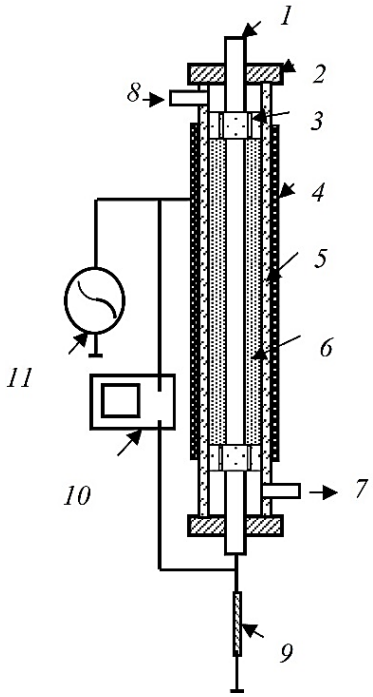

Fig. 2. DBD reactor for water solution processing. 1 – inner electrode (Al), 2 – Teflon sleeve, 3 – insulator, 4 – outer electrode (Cu foil), 5 – Pyrex tube (barrier), 6 – fiberglass coating, 7 – gas outlet, 8 – gas inlet, 9 - resistor (100 Ohm), 10 – oscilloscope GW Instek GDS-2072 (Taiwan), 11 - power supply

Рис. 2. Реактор ДБР для обработки водных растворов. 1 – внутренний электрод (Al), 2 – тефлоновая втулка, 3 –изолятор, 4 – внешний электрод (Cu фольга), 5 – пирексовая трубка (барьер), 6 – покрытие из стеклоткани, 7 – выход газа, 8 – вход газа, 9 – резистор (100 Ом), 10 – осциллограф GW Instek GDS-2072 (Taiwan), 11 – источник питания

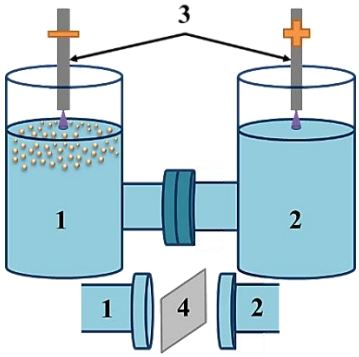

Fig. 3. The scheme of the experimental setup. 1 - liquid anode, 2 - liquid cathode, 3 - titanium electrodes, 4 – membrane

Рис. 3. Схема экспериментальной установки. 1 - жидкий анод, 2 - жидкий катод, 3 - титановые электроды, 4 – мембрана

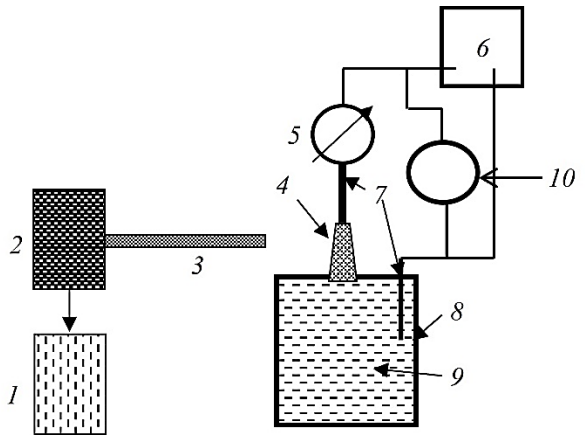

Fig. 4. The schematic diagram of the experimental setup. 1 – data acquisition system (PC), 2 – monochromator, 3 - light guide, 4 – discharge, 5 – ammeter, 6 – direct current power supply, 7 – electrodes, 8 – reaction vessel, 9 – solution, 10 – voltmeter. The solution served as the cathode (-)

Рис. 4. Принципиальная схема экспериментальной установки. 1 – система сбора данных (ПК), 2 – монохроматор, 3 – световод, 4 – разряд, 5 – амперметр, 6 – источник постоянного тока, 7 – электроды, 8 – реакционный сосуд, 9 – раствор, 10 – вольтметр. Раствор – катод (-)

METHODS OF ANALYSIS AND MEASUREMENTS

The concentrations of organochlorine compounds (OCs) (in liquid and gas phases) at the inlet and outlet of the reactor were determined by the gas chromatographic method using a Khromatek-5000 chromatograph with an electron capture detector (ZAO Khromatek, Russia). The content of naphthalene was controlled by high performance liquid chromatography (HPLC) using a Fluorat 2-M fluorimeter (OOO Lumeks, Russia). The control of monobasic carboxylic acids was carried out by the photometric method using a UNICO-2804 spectrophotometer, USA. The concentration of aldehydes was determined by the fluorimetric method. The content of oil products was controlled by fluorimetric and IR spectrometric methods (Nicolet Avatar 360, USA). The chlorine concentration in the degradation products was estimated by the potentiometric method. Determination of the content of CO and CO_2 in the gas phase was carried out by gas chromatography (Khromatek-5000) using a flame ionization detector. The CO_2 concentration in the liquid phase was controlled by a potentiometric method. The concentration of ozone formed in the discharge zone of the reactor was determined by absorption spectroscopy by light absorption at λ = 254 nm (UNICO-2804, USA). The index of chemical oxygen demand (COD) was controlled by the photometric method using a Fluorat 2-M fluorimeter.

For DC discharge, the following techniques were used. The measurement of the electric field strength (E) in the positive column and cathode potential drop (U_c) consisted in measuring the total voltage drop between the liquid and metal electrodes as a function of the cathode-anode distance [14,15]. The tangent of the slope of this dependence gives the value of E, and the segment cut off on the ordinate axis - the value of U_c. To determine the geometric dimensions of the discharge and the current densities, we used the method of photographic recording of the discharge. The discharge emission spectra in the wavelength range of 300-900 nm were recorded using an Avaspec-2048FT-2 spectrometer (Avantes, the Netherlands) with a diffraction grating of 600 lines/mm and an entrance slit width of 50 μm. The real resolution of the instrument was 1.3 nm. If it was necessary to obtain more resolved spectra, an Avaspec-3648 spectrometer with a diffraction grating of 1200 lines/mm, an entrance slit width of 10 μm, and a real resolution of 0.17 nm was used in the wavelength range of 350-400 nm. From the results of spectral measurements, the values of the effective vibrational temperature were found, which characterize the populations of the lower excited vibrational states (levels) of $N_2(C^3\Pi_u)$ nitrogen molecules. To do this, we measured the relative intensities of the electronic-vibrational bands of the $C^3\Pi_u,\rightarrow B^3\Pi_g$, V transitions [16]. To determine the temperature of the neutral component of the gas, we used a method for determining the temperature based on measuring the intensities of the rotational lines of the electronic vibrational emission bands. It is shown that, under the conditions under study, identification of the rotational temperature with the translational temperature is possible, since the distribution of molecules over the rotational levels of the excited electronic state obeys the Boltzmann distribution, and the rotational-translational relaxation has ended in the system [14].

The processes of formation of colloidal solutions and the properties of the obtained substances were studied by the following methods. Turbidimetric and nephelometric studies were used to describe the kinetics of particle formation processes in solution. The solution was illuminated with a beam of light, and then the intensity of the transmitted radiation or the intensity of the radiation scattered at an angle at 90° during the discharge was measured. A helium-neon laser with a wavelength of 632.8 nm was used as a radiation source. The laser beam was directed in such a way that the radiation passed through the solution at a distance of 1 mm from its surface; the optical length was 45 mm. To register the radiation, an AvaSpec-2048FT-2 spectrometer was used. The synthesized powder was taken separately from the bottom and from the near-surface layer of the cell, centri-

fuged and dried at a temperature of 60°C for 24 h on glass substrates. The resulting powders were subjected to X-ray phase analysis (DRON 3M, Burevestnik, Russia), the elemental composition of the powders was determined by EDX analysis (Aztec EDS, Oxford Instrumental, England), thermogravimetric analysis, and differential calorimetry (STA 449 F1 Jupiter Netzsch, Germany) were performed. The morphology and particle size of the powders were determined using scanning electron microscopy (TESCAN VEGA3 SBH, Czech Republic) and dynamic light scattering (Photocor Compact-Z, Photokor, Russia).

SIMULATION METHODS

To understand how the discharge initiates chemical processes in the solution, it is necessary to know the concentrations of active species formed in the plasma and their fluxes to the surface of the solution. The available experimental methods for measuring concentrations are extremely limited. Therefore, mathematical modeling is in this case an effective method for obtaining such information. In this work, we used an approach based on the joint solution of the Boltzmann equation for electrons, the equations of vibrational kinetics for the ground states of molecules, and the equations of chemical kinetics [17]. The current densities *j* and the reduced electric field strengths E/N (N is the total concentration of particles) required for calculation were taken from experience. For air, the initial composition of the gas phase included N_2 and O_2 molecules and Ar atoms, as well as atoms and molecules that were formed in the gas phase during discharge combustion, and H_2O molecules coming from the solution. When calculating the energy distribution functions of electrons (EEDF), collisions of the 1st and 2nd kind were taken into account: with Ar atoms in the ground and excited states $^1P_1$, $^3P_0$, $^3P_1$, $^3P_2$; with O_2 molecules in the ground state and metastable $O_2(a^1\Delta_g)$, $O_2(b^1\Sigma_g^+)$ molecules; with oxygen atoms in the ground state and excited $O(^1D,^1S, 3s^3S, 3s^5S)$; with H_2 molecules in the ground and vibrationally excited states; with H_2O molecules in the ground and vibrationally excited states; with NO molecules in the ground and vibrationally excited states. Electron-electron collisions were also taken into account. When calculating the vibrational kinetics, the excitation-de-excitation of vibrational levels by electron impact, single-quantum V-V and V-T exchange, and some chemical reactions were taken into account. The level constants of the rates of vibrational exchange were calculated from the relations of the SSH theory with normalization to experimental values, where they are known. The equations of vibrational kinetics described the vibrational energy exchange in the system of ground vibrational states of the O_2, N_2, H_2O, NO, and H_2 molecules. Since the content of H_2O molecules was not known, it was chosen in such a way as to achieve agreement between the calculation of the vibrational temperatures of the $N_2(C^3\Pi_u)$ state, the intensities of the emission bands of the N_2 second positive system (the $C^3\Pi_u \rightarrow B^3\Pi_g$ transition), the some emission intensities of the Ar lines and oxygen atoms, and the experimentally found values [17-20]. The equations of chemical kinetics for plasma included 328 reactions involving electrons, as well as ground and excited states of atoms and molecules ($O_2(X)$, $O_2(a^1\Delta)$, $O_2(b^1\Sigma)$, $O_2(A^3\Sigma)$, $O(^3P)$, $O(^1D)$, $O(^1S)$, O_3, $O(3p^3P)$, $O(3s^3S)$, H_2O, H, OH, H_2O_2, HO_2, H_2, H, $N_2(X)$, N_2O, NO, NO_2, NO_3, HNO, HNO_2, HNO_3, $N_2(X)$, $N_2(A^3\Sigma_u^+)$, $N_2(B^3\Pi g)$, $N_2(C^3\Pi u)$, $N_2(a'^1\Sigma^+)$, Ar(X), Ar ($^1P_1$,$^3P_0$,$^3P_1$,$^3P_2$) A list of these reactions is given in work [20].

The chemical kinetics equations for solutions included 28 components (H_2O, H_2O_2, OH, HO_2, HNO_3, HNO_2, HO_3, O_3, O_2, H, H_2, NO, NO_2, NO_3, e_{aq} (solvated electron), ONOOH, O, H^+, OH^-,O^-, O_2^-, HO_2^-, O_2^-, NO_3^-, NO_2^-, O_3^-,O_2^{2-}, NO_2^{2-}) and 119 reactions between them [21]. This system of stiff kinetic equations was solved by the 5th order Gear method [22] with boundary conditions in the form of a flow of the corresponding particles from the plasma at the plasma-solution interface.

DEGRADATION OF TOXIC COMPOUNDS

The studied substances were highly toxic, persistent compounds (chlorinated organic compounds (tetrachloromethane (TCM), 1,4-dichlorobenzene (1,4-DCB), 2,4-dichlorophenol (2,4-DCP)). The concentrations of the studied compounds in water were: 2,4-DCP – 5 - 100 mg/l (62-616 μmol/l); TCM - 5 - 100 mg/l (6.5 - 650 μmol/l). The concentrations of the studied compounds in the gas phase were: 2,4-DCP - 0.06 - 1.0 g/m^3 (368 - 6134 μmol/l); 1,4-DCB - 0.076 - 0.382 g/m^3 (517 - 2599 μmol/l); TCM - 0.03 - 1.65 g/m^3 (194 - 10714 μmol/l). In all cases, the plasma-forming gas was oxygen (99.8%).

KINETICS OF DESTRUCTION OF VAPOR-GAS MIXTURES

Studies have shown that the kinetics of the destruction of CCl4, 2,4-DCP, 1,4-DCB (dependence of the concentration at the outlet of the reactor as a function of the residence time of gas in the discharge zone) is well described by a formal equation of the first kinetic order (determination coefficient R2 > 0.95) (see, for example, Fig. 5) [23-25].

Some rate constants and decomposition rates are presented in Table 1. Rates correspond to contact times tending to zero. The effective rate constants decrease with increasing concentration at the reactor inlet, however, the decrease is slower than the increase in concentration, which leads to an increase in the rate of decomposition and the energy efficiency of the process, however, a decrease in the degree of decomposition is observed. The degrees of decomposition of substances decrease with increasing their concentration. In general, the degrees of decomposition of all the investigated substances reach values of 0.8-1.

When cleaning vapor-gas mixtures, it is important not only to obtain a high degree of decomposition of the target substance, but also to know the composition of the resulting products. At a degree of TCM decomposition of 0.99 (concentration at the inlet is 195 mmol/m^3, power is 1 W/cm^3, residence time is 4.2 s), chloroform ($CHCl_3$), 1,2-dichloroethane (CH_2Cl-CH_2Cl) and trichlorethylene (CCl_2=$CHCl$) were found with concentrations less than 0.01 mmol/m^3. The main decomposition products were CO_2 and Cl_2 molecules with a yield of about 90%. Approximately the same situation with products is observed for 1,4-DCB and 2,4-DCP. The main decomposition products are CO_2 and Cl_2 molecules. Small amounts of carboxylic acids and aldehydes are also formed.

Thus, the dielectric barrier discharge of atmospheric pressure is an effective method of destruction of chlorine-containing compounds in gas mixtures (decomposition degree up to 100% under certain conditions) at low energy costs. The main decomposition products are CO_2 and Cl_2, which are easily neutralized by simple chemical methods into non-toxic carbonates (CO_3^{2-}) and chlorides (Cl^-).

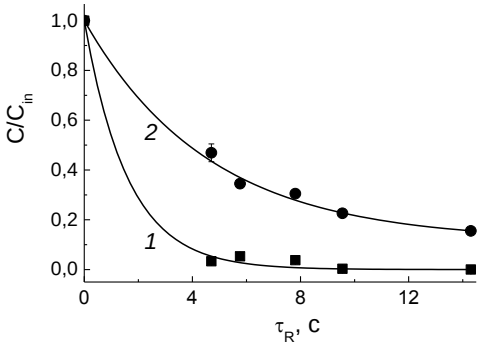

Fig. 5. Dependence of the concentration of TCM at the outlet of the DBR reactor on the residence time of the gas with the discharge zone. Specific power is 1 W/cm^3. 1, 2 - TCM concentrations at the reactor inlet (C_{in}) are 30 mg/m^3 and 1.65 g/m^3, respectively. Points - experiment. Lines - calculation according to the equation of the 1st kinetic order

Рис. 5. Зависимость концентрации ТХМ на выходе из реактора ДБР от времени контакта газа с зоной разряда. Удельная мощность 1 Вт. 1, 2 - концентрации ТХМ на входе в реактор (C_{in}) 30 мг/м^3 и 1.65 г/м^3 соответственно. Точки - эксперимент. Линии – расчет по уравнению 1-го кинетического порядка

Kinetics of destruction in water solution

As for the gas phase, the decomposition kinetics of TCM and 2,4-DCP in their aqueous solutions is well described ($R^2 > 0.98$) by the equation of the first kinetic order with respect to the concentration of the target substance [26-28].

Table 1

Decomposition characteristics of chlorinated derivatives [23-25]. Power is 0.8 W/cm^3

***Таблица 1.* Характеристики разложения хлорпроизводных [23-25]. Мощность 0,8 Вт/см^3**

Substance	Reactor inlet concentration, g/m^3	Decomposition rate, cm^{-3}·s^{-1}	Rate constant, s^{-1}	Energy efficiency	
				mol/100 eV	kJ/l
CCl_4	0.03	$0.7\cdot10^{14}$	0.59±0.08	0.0010	2.9
	1.65	$10.1\cdot10^{14}$	0.16±0.02	0.0120	14.5
2,4-dichlorophenol	1.0	$4.4\cdot10^{14}$	0.22±0.03	0.0035	18.9
1,4-dichlorobenzene	0.3	$2.0\cdot10^{14}$	0.13±0.05	0.0027	24.0

Table 2

Decomposition characteristics of chlorinated derivatives in water solutions [26-28]

***Таблица 2.* Характеристики разложения хлорпроизводных в водных растворах [26-28]**

Reactor inlet concentration, mol/l	Decomposition rate, mol/(l·s)	Rate constant, s^{-1}	Energy efficiency molecules/100 eV
CCl_4, (power) 5 Вт			
$3.25\cdot10^{-4}$	0.000584	4.89 ± 0.08	1.34
$1.95\cdot10^{-4}$	0.000319	4.45 ± 0.03	0.78
$9.75\cdot10^{-5}$	0.000197	5.48 ± 0.19	0.40
$3.25\cdot10^{-5}$	0.000067	5.61 ± 0.29	0.14
2,4-ДХФ (2,4-DCP), (power) 10.4 Вт			
$6.2\cdot10^{-5}$	0.00005	2.17±0.17	0.04
$9.3\cdot10^{-5}$	0.00006	1.90±0.10	0.05
$3.08\cdot10^{-4}$	0.00023	2.00±0.15	0.17

Effective constants, decomposition rates and energy efficiencies are shown in Table 2. The energy efficiency of 2,4-DCP degradation is significantly higher than that of TCM, i.e., aromatic compounds are more stable than aliphatic chlorinated hydrocarbons. Comparing the efficiency of 2,4-DCP decomposition processes in the liquid phase with similar processes in the gas phase (Table 1), we can conclude that in the gas phase they are less efficient by about an order of magnitude. The degree of decomposition achieved for both compounds is close to unity.

During the decomposition of TCM, the presence of small amounts of aldehydes and chloride ions in solution was found. CO_2 and CO molecules are registered in the gas phase. Almost all carbon in CO and CO_2 corresponds to the amount of decomposed TCM, as well as the amount of Cl- ions in the solution.

Experiments have shown that the decomposition of 2,4-DCP in solution produces carboxylic acids and aldehydes, and carbon dioxide is formed in the gas phase. The chlorine formed during decomposition is represented by Cl_2 molecules in the gas phase and Cl- ions in solution.

PARAMETERS OF DC DISCHARGES AND CONCENTRATIONS OF ACTIVE SPECIES [17-20, 29]

Plasma physical parameters

In all studied plasma-forming gases (O_2, N_2, Ar, air), the discharge has the form of a cone-shaped luminous column. In this column, a number of areas characteristic of a glow discharge can be distinguished: the region of the anode glow, the positive column of the discharge, the dark cathode space, and the cathode glow. In the wavelength range of 200-400 nm, the spectral composition of the radiation is qualitatively the same for all the studied gases. Emission bands of the NO γ-system ($A^2\Sigma \rightarrow X^2\Pi$ transition), OH-radical ($A^2\Sigma \rightarrow X^2\Pi$ transition) and the second positive N_2 system ($C^3\Pi u \rightarrow B^3\Pi g$ transition) are observed in this region. Only the absolute emission intensities of the bands of the listed components differ. The presence of NO and OH emission bands, as well as hydrogen lines in argon, nitrogen, and oxygen plasmas, is associated with the transfer of liquid cathode decomposition products into the gas phase—hydrogen and oxygen atoms or molecules and hydroxyl radicals. The presence of weak emission bands of the second positive nitrogen system in pure argon and oxygen is associated with the transition to the gas phase of nitrogen molecules dissolved in water. The long-wave part of the spectrum is individual for each working gas. For oxygen and air plasmas, these are emission lines of atomic oxygen; for argon plasma, these are emission lines Ar.

The measured dependences of the cathodic potential drop, the reduced electric field strengths, the powers put into the discharge, the gas temperatures, and the vibrational temperatures on the pressure of the plasma-forming gas are shown in Figs. 6-10.

For the studied molecular plasma-forming gases, the mechanisms of gas heating are considered. It has been established that in all molecular gases, the heating of the gas is due to the processes of transferring the energy of vibrational excitation of molecules (VEM) into thermal energy (V-T relaxation). In oxygen plasma, the characteristic V-T relaxation times are much shorter than the diffusion residence times of the VEM for the plasma zone. For plasmas of air and nitrogen, the opposite picture is observed. Therefore, in O_2 plasma, almost all the energy deposited in the VEM is released in the plasma zone, while for a discharge in air and nitrogen, a significant part of the energy is carried out by the VEM outside the discharge zone. This feature determines higher temperatures for O_2 plasma. For a discharge in nitrogen and in air, it is shown that vibrationally excited nitrogen molecules in the ground state have a strong effect on the EEDF due to superelastic collisions with electrons.

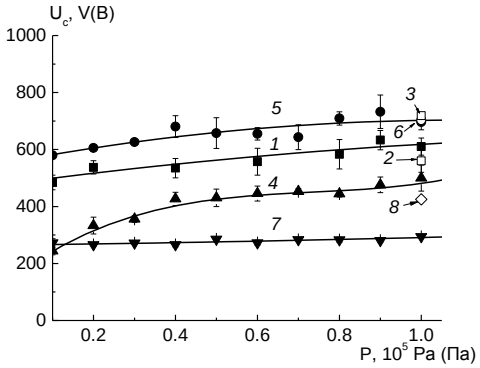

Fig. 6. Cathodic potential drop vs pressure. I_p=40 mA: 1,2,3 - air; 4 - O_2; 5,6 - N_2; 7,8 – Ar. 2,3,6,8 - literature data

Рис. 6. Катодное падение потенциала как функция давления. I_p=40 мА: 1,2,3 – воздух; 4 – O_2; 5,6 – N_2; 7,8 – Ar: 2,3,6,8 – данные литературы

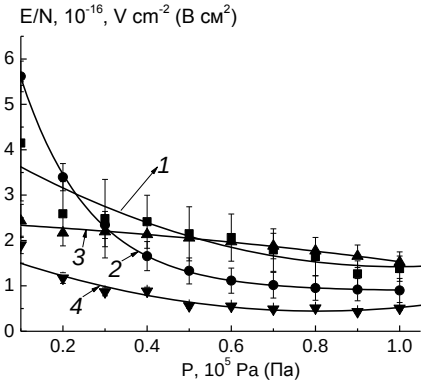

Fig. 7. Reduced electric field strength in the positive discharge column as a function of pressure. I_p=40 mA. 1 – air; 2 - N_2; 3 - O_2; 4 - Ar

Рис. 7. Приведенная напряженность электрического поля в положительном столбе разряда как функция давления. I_p=40 мА: 1 – воздух; 2 – N_2; 3 – O_2; 4 – Ar

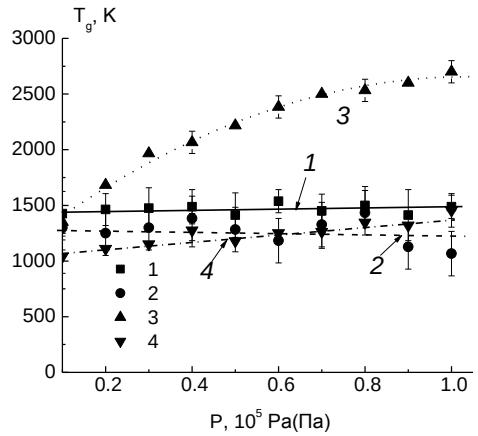

Fig. 8. Gas temperatures (T_g) as a function of pressure. I_p=40 mA: 1 – air; 2 - N_2; 3 - O_2; 4-Ar

Рис. 8. Газовые температуры (T_g) как функции давления. I_p=40 мА: 1 – воздух; 2 – N_2; 3 – O_2; 4 – Ar

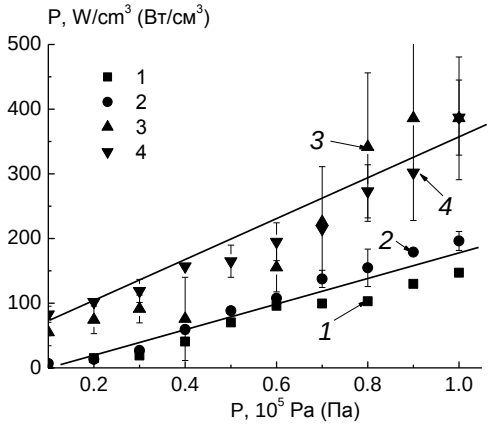

Fig. 9. Power deposited in the discharge as a function of pressure. I_p=40 mA: 1 – air; 2 - N_2; 3 - O_2; 4-Ar

Рис. 9. Вкладываемая в разряд мощность как функция давления. I_p=40 мА: 1 – воздух; 2 – N_2; 3 – O_2; 4 – Ar

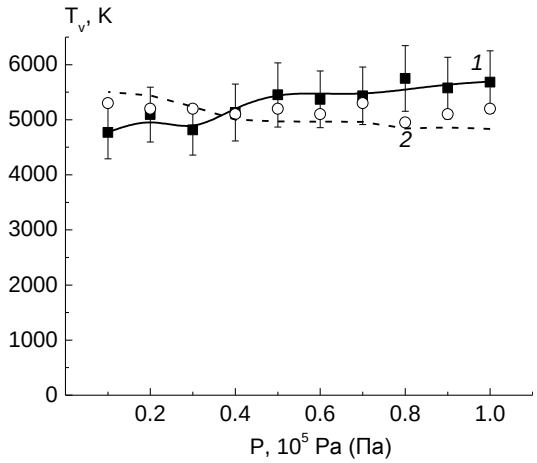

Fig. 10. Calculated and measured vibrational temperature of $N_2(C^3\Pi_u)$ as a function of pressure. I_p=40 mA.: 1 – air; 2 - N_2. Points - experiment, lines – calculation

Рис. 10. Расчетная и измеренная колебательная температура $N_2(C^3\Pi_u)$ как функция давления. I_p=40 мА.: 1 – воздух; 2 – N_2. Точки - эксперимент, линии – расчет

Chemical composition of plasma

Modeling of the plasma composition showed that the qualitative composition of the formed particles is the same regardless of the type of plasma-forming gas. The main oxygen-containing species are H_2O, OH, H_2O_2, $O(^3P)$ and HO_2. Discharge plasmas in oxygen and air also contain a significant number of metastable states $O_2(a^1\Delta g)$ and $O_2(b^1\Sigma^+ g)$. When discharged in air, NO, NO_2, N_2O, HNO_2 HNO_3 molecules are also formed. Figs 11-14 show the dependences of the concentrations of the main neutral components in air plasma on pressure.

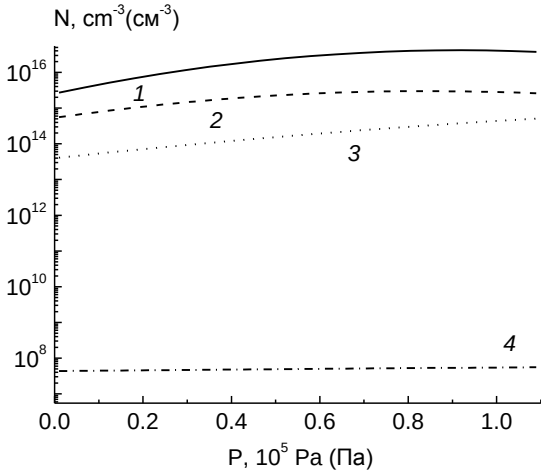

Fig. 11. The concentration of nitrogen oxide molecules in the discharge in air as a function of pressure. I_p = 40 mA. 1 - NO; 2 - NO_2; 3 - N_2O; 4 - NO_3

Рис. 11. Концентрации молекул оксидов азота в разряде в воздухе как функция давления. I_p=40 мА. 1 – NO; 2 – NO_2; 3 – N_2O; 4 – NO_3

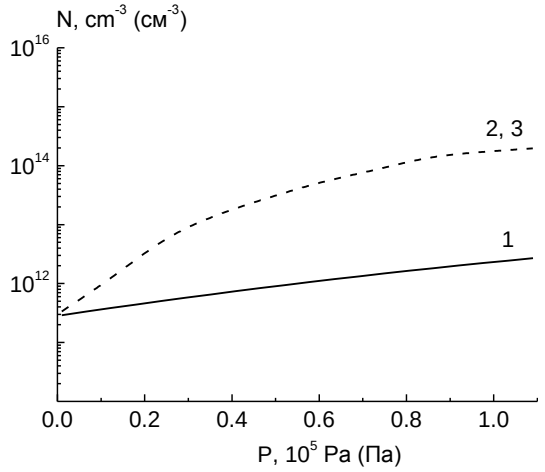

Fig. 12. Concentrations of HNO_2, HNO_3 and HNO molecules in a discharge in air as a function of pressure. I_p=40 mA: 1 – HNO_3; 2 - HNO_2; 3-HNO

Рис. 12. Концентрации молекул HNO_2, HNO_3 и HNO в разряде в воздухе как функция давления. I_p=40 мА: 1 – HNO_3; 2 – HNO_2; 3 – HNO

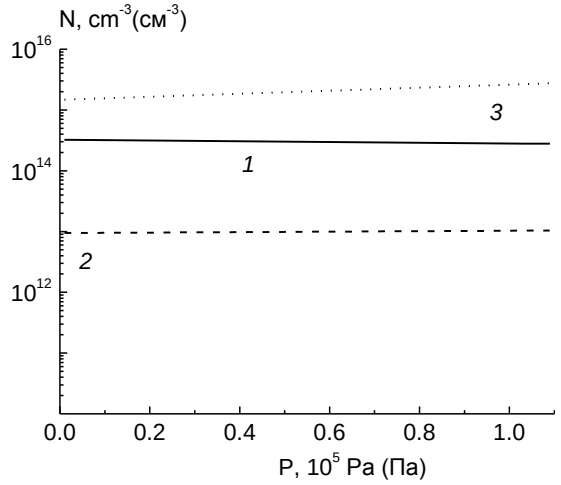

Fig. 13. Concentrations of H_2O_2 molecules and OH and HO_2 radicals in air as a function of pressure. I_p=40 mA: 1 – H_2O_2; 2 - HO_2; 3-OH

Рис. 13. Концентрации молекул H_2O_2 и радикалов OH и HO_2 в воздухе как функция давления. I_p=40 мА: 1 – H_2O_2; 2 – HO_2; 3 – OH

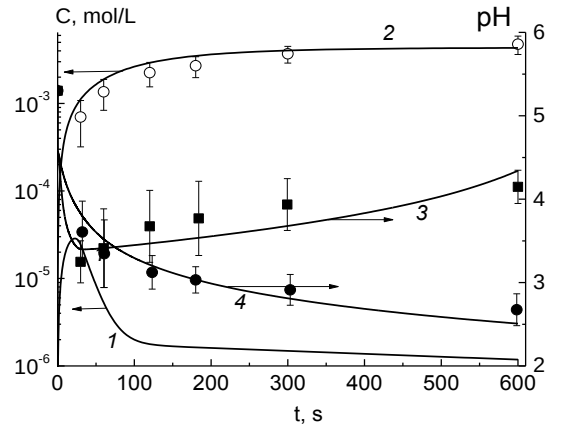

Fig. 14. Hydrogen peroxide concentrations (1,2) and solution pH (3.4) as functions of time for discharge in air at a current of 40 mA. Points - experiment, lines – calculation. 1, 3 – liquid cathode. 2, 4 – liquid anode

Рис. 14. Концентрации пероксида водорода (1,2) и pH раствора (3,4) как функции времени для разряда в воздухе при токе 40 мА. Точки - эксперимент, линии – расчет. 1, 3 – жидкий катод. 2, 4 – жидкий анод

CHEMICAL TRANSFORMATIONS IN AQUEOUS SOLUTIONS INITIATED BY THE ACTION OF A DISCHARGE

To understand the possibilities of using a solution activated by the action of a discharge, information is needed on the types and concentrations of active particles formed in the solution. And the determination of the main reactions of formation and decay of particles is of interest from the point of view of predicting changes in the properties of the solution with changes in the discharge parameters. Unfortunately, the possibilities of experimental methods for determining the concentrations of short-lived particles, such as radicals, are severely limited. For example, the use of radical scavengers is hindered by the fact that, due to the complex chemical composition of the solution, the scavengers, as well as the substances obtained from them (which are identified), can react simultaneously with several components of the solution. Experimental data are available for hydrogen peroxide concentrations, pH values, and nitrite and nitrate ion concentrations [21]. For this reason, mathematical modeling actually becomes a tool for studying the composition of a solution and the mechanisms of reactions occurring in it.

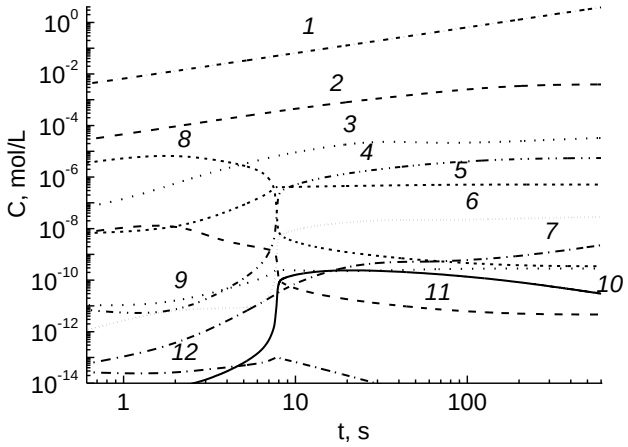

Fig. 15. Changes in the concentration of components over time. 1-12: O_2, H_2, HNO_2, HO_2, ONOOH, NO_2, HNO_3, NO, OH, O^{2-}, O_3, O^-, respectively. Gas is air. Discharge current 40 mA. Solution is cathode

Рис. 15. Изменение концентрации компонентов во времени. 1-12: O_2, H_2, HNO_2, HO_2, ONOOH, NO_2, HNO_3, NO, OH, O^{2-}, O_3, O^- соответственно. Газ – воздух. Ток разряда 40 мА. Раствор – катод

The concentrations of the solution components obtained in the experiment and during simulation for a direct current discharge in air are shown in Fig. 14, 15. The results of calculations of the fluxes of the main components from the discharge to the solution surface showed that they differ not too much for both the liquid cathode and the liquid anode. And the differences in the kinetics and concentrations of species in the solution are due to the fact that in the liquid cathode, unlike the anode, there is a channel for the formation of hydrogen peroxide, due to the bombardment of the solution surface by positive ions accelerated in the cathode potential drop. This leads to the fact that the concentration of hydrogen peroxide in the liquid anode is at least two orders of magnitude lower than in the liquid cathode. This explains the higher efficiency of the liquid cathode compared to the anode in the

reduction reactions Cr(VI) and Mn(VII), where hydrogen peroxide plays the main role due to the reactions $Cr_2O_7^-$+ $8H^+$+H_2O_2→$2Cr^{3+}$+$5H_2O$+$2O_2$ and $2MnO_4^-$+ $6H^+$+$5H_2O_2$→$2Mn^{2+}$+$8H_2O$+$5O_2$ (stoichiometric equations, acidic environment) [30-36]. The decomposition of H_2O_2 with the formation of OH radicals provides a significantly higher concentration of OH in the liquid cathode. For this reason, it can be expected that the processes of oxidative degradation of organic compounds in a liquid cathode will be more efficient. But we are not aware of such studies. In the liquid anode, the concentrations of NO and NO_2^- ions are higher than in the liquid cathode, while the concentrations of NO_3^- ions are close. For a liquid cathode and an anode, the dependences of the pH of the solution on the treatment time differ fundamentally. If in the first case, pH monotonically decreases with increasing time, and then in the second case, after passing through the minimum, an increase in pH is observed. The reason for the increase in pH is associated with the formation of solvated electrons due to the bombardment of the liquid anode by plasma electrons. The reactions of these electrons decrease the concentration of H^+ ions and increase the concentration of OH^- ions, which leads to an increase in pH. Such changes in pH explain the predominant formation of metal hydroxy compounds in solution, which is the anode. An increase in the pH of the solution ensures an increase in the concentration of OH^- ions. When the solubility limit is reached, insoluble particles of the corresponding compound are formed. Indeed, the experiment [37-42] shows that when a discharge acts on a liquid anode containing salts of cations Zn^{2+}, Cd^{2+}, Fe^{3+}, Cu^{2+}, colloidal solutions are first formed, the destruction of which leads to the formation of precipitates. The resulting colloidal particles have both a crystalline structure (compounds of zinc, cadmium, copper) and amorphous (in the case of iron). The resulting structures are mainly hydroxo compounds, oxides and hydroxides. So, for solutions of copper nitrates, these are ruatite ($Cu_2(NO_3)(OH)_3$) and copper oxide (CuO, monoclinic). In solutions of cadmium nitrate, crystalline $Cd(NO_3)(OH)_2 \cdot H_2O$, β, and γ $Cd(OH)_2$ are formed. The calcination of all precipitates obtained in an air atmosphere leads to the formation of the corresponding oxides.

The resulting colloidal particles form from two to three fractions, depending on their size. The average size of one of the fractions is in the nanometer range. A typical particle size distribution is shown in Fig. 16.

The process of formation of colloidal particles has its own kinetics. A typical dependence of the light transmission of a solution on the plasma treatment time is shown in Fig. 17. In the semi-logarithmic coordinates, two linear dependences are clearly observed. The processing allows one to determine effective rate constants or characteristic times.

These data show that the formation of colloidal particles and their subsequent sedimentation includes two stages. The first slow stage (the induction period) points to a threshold nature of the process. A particular critical concentration of particles is required to start the process, leading to their coagulation (the so-called coagulation limit). The magnitude of the induction period depends on the discharge current and initial concentration: the higher the current and concentration, the less the induction period.

Obtained in this way oxide materials have semiconductor properties, high specific surface area and catalytic properties.

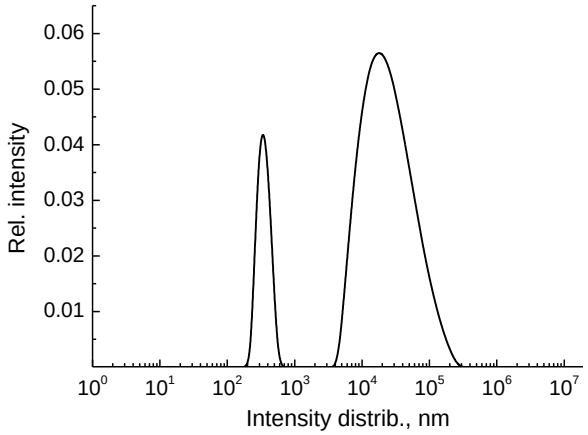

Fig. 16. Spectrum of dynamic light scattering for particles of a colloidal solution obtained from cadmium nitrate

Рис. 16. Спектр динамического рассеяния света для частиц коллоидного раствора, полученного из нитрата кадмия

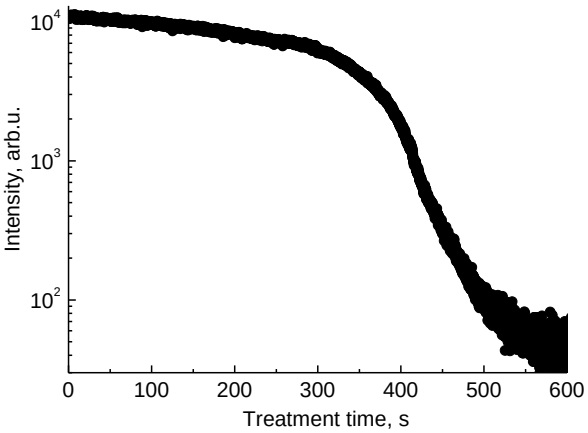

Fig. 17. The dependence of the normalized light transmission of the $Cu(NO_3)_2$ solution on the processing time. Discharge current is 40 mA. Initial concentration is 0.005 mol·L^{-1}

Рис. 17. Зависимость нормированного светопропускания раствора $Cu(NO_3)_2$ от времени обработки. Ток разряда 40 мА. Начальная концентрация 0,005 моль·$л^{-1}$

CONCLUSION

Thus, atmospheric pressure gas discharges are an effective way to purify gases and aqueous solutions from organic and inorganic contaminants. Along with the purification of aqueous solutions from heavy metal cations, nanometer-sized oxide materials can be obtained. These materials can be used as semiconductors and catalysts.

ACKNOWLEDGEMENTS

This work was supported by the Ministry of High Education and Science of the Russian Federation, project FZZW-2023-0010.

The authors declare the absence a conflict of interest warranting disclosure in this article.

The study was carried out using the resources of the Center for Shared Use of Scientific Equipment of the ISUCT (with the support of the Ministry of Science and Higher Education of Russia, No. 075-15-2021-671).

Работа поддержана Министерством высшего образования и науки Российской Федерации, проект FZZW-2023-0010.

Исследование выполнено с использованием ресурсов Центра коллективного пользования научной аппаратурой ИГХТУ (при поддержке Минобрнауки России, № 075-15-2021-671).

Авторы заявляют об отсутствии конфликта интересов, требующего раскрытия в данной статье.

REFERENCES
ЛИТЕРАТУРА

1. **Bruggeman P.J., M. Kushner M.J., Locke B.R., Gardeniers J.D.E., Graham W.G., Graves B., Hofman-Caris R.C., Maric D., Reid J.P., Ceriani E., Fernandez Riva D., J. Foster J.E., Garrick S.C., Gorbanev Y., Hamaguchi S., Iza F., Jablonowski H., Klimova E., Kolb J., Krcma F., Lukes P., Machala Z., Marinov I., Mariotti D., Mededovic Thagard S., D Minakata D., Neyts E.C., Pawlat J., Petrovic Z.L., Pflieger R., Reuter S., Schram D.C., Schröter S., Shiraiwa M., Tarabová B., Tsai P.A., Verlet J.R.R, von Woedtke T., Wilson K.R., Yasui K., Zvereva G.** // *Plasma Sources Sci. Technol.* 2016. V. 25. N 5. P. 053002. DOI: 10.1088/0963-0252/25/5/053002.
2. **Rybkin V.V., Shutov D.A.** // *Plasma Phys. Rep.* 2017. V.43. N 11. P. 1089-1113. DOI: 10.1134/S1063780X17110071.
3. **Adamovich I., Agarwal S., Ahedo E., Alves L.L., Baalrud S., Babaeva N., Bogaerts A., Bourdon A., Bruggeman P.J., Canal C., Choi E.H., Coulombe S., Donkó Z., Graves D.B., Hamaguchi S., Hegemann D., Hori M., Kim H.H., Kroesen G.M.W., Kushner M.J., Laricchiuta A., Li X., Magin T.E., Mededovic Thagard S., Miller V., Murphy A.B., Oehrlein G.S., Puac N., Sankaran R.M., Samukawa S., Shiratani M., Šimek M., Tarasenko N., Terashima K., Thomas Jr E., Trieschmann J., Tsikata S., Turner M.M., van der Walt I.J., van de Sanden M.C.M., von Woedtke T.** // *J. Phys. D: Appl. Phys.* 2022. V. 55. N 37. P. 373001. DOI:10.1088/1361-6463/ac5e1c.
4. **Choukourov A., Manukyan A.S., Shutov D.A., Rybkin V.V.** // *ChemChemTech.[Izv. Vyssh. Uchebn. Zaved. Khim. Khim. Tekhnol.]*. 2016. V. 59. N 12. P. 5-16. **Шукуров А., Манукян А.С., Шутов Д.А., Рыбкин В.В.** // *Изв. вузов. Химия и хим. технология.* 2016. Т. 59. Вып. 12. С. 5-16. DOI: 10.6060/tcct.20165912.5413.
5. **Laroussi M.** // *Front. Phys.* 2020. V. 8. N 74. P. 1-7. DOI: 10.3389/fphy.2020.00074.
6. **Laroussi M.** // *Plasma*. 2018. V. 1. N 1. P. 47-60. DOI: 10.3390/plasma1010005.
7. **Choi H.S., Rybkin V.V., Titov V.A., Shikova T.G., Ageeva T.A.** // *Surf. Coat. Technol.* 2006. V. 200. N 14-15. P. 4479-4488. DOI: 10.1016/j.surfcoat.2005.03.037.
8. **Titov V.A., Rybkin V.V., Shikova T.G., Ageeva T.A., Golubchikov O.A., Choi H.S.** // *Surf. Coat. Technol.* 2005. V. 199. N 2-3. P. 231-236. DOI: 10.1016/j.surfcoat.2005.01.037.
9. **Chokradjaroen C., Wang X., Niu J., Fan T., Saito N.** // *Mater. Today Adv.* 2022. V. 14. P. 100244. DOI: 10.1016/j.mtadv.2022.100244.
10. **Foster J.E.** // *Phys. Plasmas.* 2017. V. 24. N 5. P. 055501. DOI: 10.1063/1.4977921.
11. **Misra N.N.** // *Trends Food Sci. Technol.* 2015. V. 45. N 2. P. 229-244. DOI: 10.1016/j.tifs.2015.06.005.
12. **Mu R., Liu Y., Li R., Xue G., Ognier S.** // *Chem. Eng. J.* 2016. V. 296. N 2-3. P. 356-365. DOI: 10.1016/j.cej.2016.03.106.
13. **Ivanov A.N., Shutov D.A. Manukyan A.S., Rybkin V.V.** // *Plasma Chem. Plasma Process.* 2018 V. 33. N 4. P. 63-73. DOI: 10.1007/s11090-018-9936-9.
14. **Titov V.A., Rybkin V.V., Maximov A.I., Choi H.-S.** // *Plasma Chem. Plasma Process.* 2005. V. 25. N 5. P. 503-518. DOI: 10.1007/s11090-005-4996-z.
15. **Shutov D.A., Artyukhov A.I., Ivanov A.N., Rybkin V.V.** // *Plasma Phys. Rep.* 2019. V. 45. N 11. P. 997–1004. DOI: 10.1134/S1063780X19100052.
16. **Titov V.A., Rybkin V.V., Smirnov S.A., Kulentsan A.L., Choi H.-S.** // *Plasma Chem. Plasma Process.* 2006. V. 26. N 5. P. 543-555. DOI: 10.1007/s11090-006-9014-6.
17. **Smirnov S.A., Shutov D.A., Bobkova E.S., Rybkin V.V.** // *Plasma Chem. Plasma Process.* 2015. V. 35. N 4. P. 639–657. DOI: 10.1007/s11090-015-9626-9.
18. **Bobkova E.S., Smirnov S.A., Zalipaeva Ya.V., Rybkin V.V.** // *Plasma Chem. Plasma Process*. 2014. V. 34. N 4. P. 721–743. DOI: 10.1007/s11090-014-9539-z.
19. **Smirnov S.A., Shutov D.A., Bobkova E.S., Rybkin V.V.** // *Plasma Chem. Plasma Process.* 2016. V. 36. N 2. P. 415–436. DOI: 10.1007/s11090-015-9669-y.
20. **Shutov D.A., Smirnov S.A., Bobkova E.S., Rybkin V.V.** // *Plasma Chem. Plasma Process.* 2015. V. 35. N 1. P. 107–132. DOI: 10.1007/s11090-014-9596-3.
21. **Shutov D.A., Batova N.A., Smirnova K.V., Ivanov A.N., Rybkin V.V.** // *J. Phys. D: Appl. Phys.* 2022. 55. N 34. P. 345206. DOI: 10.1088/1361-6463/ac74f8.
22. **Gear C.W.** Numerical Initial Value Problems in Ordinary Differential Equations. Englewood Cliffs, NJ: Prentice-Hall. 1971. 253 p.
23. **Gushchin A.A., Grinevich V.I., Izvekova T.V., Kvitkova E.Yu., Tyukanova K.A., Rybkin V.V.** // *Int. J. Environ. Sci. Technol.* 2020. V. 17. P. 3449–3458. DOI: 10.1007/s13762-020-02703-2.
24. **Gushchin A.A., Grinevich V.I., Kozlov A.A., Kvitkova E.Yu., Shutov D.A., Rybkin V.V.** // *Plasma Chem.*

Plasma Process. 2017. V. 37. N 5. P. 1331-1341. DOI: 10.1007/s11090-017-9828-4.
25. **Gushchin A.A., Grinevich V.I., Izvekova T.V., Kvitkova E.Yu., Tyukanova K.A., Rybkin V.V.** // *Chemosphere*. 2021. V. 270. P. 129392. DOI: 10.1016/j.chemosphere.2020.129392.
26. **Gushchin A.A., Grinevich V.I., Izvekova T.V., Kvitkova E.Yu., Tyukanova K.A., Rybkin V.V.** // *Plasma Chem. Plasma Process.* 2019. V. 39. N 2. P. 461–473. DOI: 10.1007/s11090-019-09958-9.
27. **Gushchin A.A., Grinevich V.I., Shulyk V.Ya., Kvitkova E.Yu., Rybkin V.V.** // *Plasma Chem. Plasma Process.* 2018. V. 38. N 1. P. 123–134. DOI: 10.1007/s11090-017-9857-z.
28. **Gusev G.I., Gushchin A.A., Grinevich V.I., Izvekova T.V., Sharonov A.V., Rybkin V.V.** // *ChemChemTech. [Izv. Vyssh. Uchebn. Zaved. Khim. Khim. Tekhnol.]*. 2020. V. 63. N 7. P. 88-94. **Гусев Г.И., Гущин А.А., Гриневич В.И., Извекова Т.В., Шаронов А.В., Рыбкин В.В.** // *Изв. вузов. Химия и хим. технология.* 2020. Т. 63. Вып. 7. С. 88-94. DOI: 10.6060/ivkkt.20206307.6182.
29. **Bobkova E.S., Khodor Ya.V., Kornilova O.N., Rybkin V.V.** // *High Temp.* 2014. V. 52. N 4. P. 511 – 517. DOI: 10.1134/S0018151X14030055.
30. **Smirnova K.V., Ivanov A.N., Shutov D.A., Manukyan A.S., Rybkin V.V.** // *Russ. J. Neorg. Chem.* 2022. V. 67. N 3. P. 262-266. **Смирнова К.В., Иванов А.Н., Шутов Д.А., Манукян А.С., Рыбкин В.В.** // *Журн. Неорг. Химии*. 2022. Т. 67. N 3. С. 262-266. DOI: 10.1134/S0036023622030123.
31. **Shutov D.A., Batova N.A., Rybkin V.V.** // *High Energy Chem.* 2020. V. 54. N 1. P. 59-63. **Шутов Д.А., Батова Н.А., Рыбкин В.В.** // *Химия Высоких Энергий.* 2020. Т. 54. N 1. С. 59-63. DOI: 10.1134/S0018143920010117.
32. **Shutov D.A., Sungurova A.V., Manukyan A.S., Izvekova A.A., Rybkin V.V.** // *High Energy Chem.* 2019. V. 53. N 5. P. 385-389. **Шутов Д.А., Сунгурова А.В., Манукян А.С., Извекова А.А., Рыбкин В.В.** // *Химия Высоких Энергий.* 2019. Т. 53. N 5. С. 385-389. DOI: 10.1134/S0018143919050126.
33. **Shutov D.A., Sungurova A.V., Manukyan A.S., Rybkin V.V.** // *High Energy Chem.* 2018. V. 52. N 2. P. 429-432. **Шутов Д.А., Сунгурова А.В., Манукян А.С., Рыбкин В.В.** // *Химия Высоких Энергий.* 2018. Т. 52. N 2. С. 429-432. DOI: 10.1134/S0018143918050144.
34. **Shutov D.A., Sungurova A.V., Smirnova K.V., Manukyan A.S., Rybkin V.V.** // *ChemChemTech [Izv. Vyssh. Uchebn. Zaved. Khim. Khim. Tekhnol.]*. 2018. V. 61. N 9-10. P. 24-30. **Шутов Д.А., Сунгурова А.В., Смирнова К.С., Манукян А.С., Рыбкин В.В.** // *Изв. вузов. Химия и хим. технология.* 2018. Т. 61. Вып. 9-10. С. 24-30. DOI: 10.6060/ivkkt20186109-10.5802.
35. **Shutov D.A., Sungurova A.V., Smirnova K.V., Rybkin V.V.** // *High Energy Chem.* 2018. V. 52. N 1. P. 95-98. DOI: 10.1134/S0018143918010125.
36. **Shutov D.A., Sungurova A.V., Choukourov A., Rybkin V.V.** // *Plasma Chem. Plasma Process*. 2015. V. 36. N 5. P. 1253-1269. DOI: 10.1007/s11090-016-9725-2.
37. **Shutov D.A., Smirnova K.V., Ivanov A.N., Rybkin V.V.** // *Plasma Chem. Plasma Process.* 2022. V. 42. N 1. P. 179-190. DOI: 10.1007/s11090-021-10208-0.
38. **Smirnova K.V., Shutov D.A., Ivanov A.N., Manukyan A.S., Rybkin V.V.** // *ChemChemTech [Izv. Vyssh. Uchebn. Zaved. Khim. Khim. Tekhnol.]*. 2022. V. 65. N 7. P. 28-34. **Смирнова К.В., Шутов Д.А., Иванов А.Н., Манукян А.С., Рыбкин В.В.** // *Изв. вузов. Химия и хим. технология.* 2022. Т. 65. Вып. 7. С. 28-34. DOI: 10.6060/ivkkt.20226507.6629.
39. **Smirnova K.V., Shutov D.A., Ivanov A.N., Manukyan A.S., Rybkin V.V.** // *ChemChemTech [Izv. Vyssh. Uchebn. Zaved. Khim. Khim. Tekhnol.]*. 2021. V. 64. N 7. P. 83-88. **Смирнова К.В., Шутов Д.А., Иванов А.Н., Манукян А.С., Рыбкин В.В.** // *Изв. вузов. Химия и хим. технология.* 2021. Т. 64. Вып. 7. С. 83-88. DOI: 10.6060/ivkkt.20216407.6409.
40. **Shutov D.A., Ivanov A.N., Rakovskaya A.V., Smirnova K.V., Manukyan A.S., Rybkin V.V.** // *J. Phys. D: Appl. Phys.* 2020. V. 53. N 44. P. 445202. DOI: 10.1088/1361-6463/aba4d7.
41. **Shutov D.A., Smirnova K.V., Gromov M.V., Ivanov A.N., Rybkin V.V.** // *Plasma Chem. Plasma Process.* 2018. V. 38. N 1. P. 107-121. DOI: 10.1007/s11090-017-9856-0.
42. **Shutov D.A., Rybkin V.V., Ivanov A.N., Smirnova K.V.** // *High Energy Chem.* 2017. V. 51. N 1. P. 65-69. **Шутов Д.А., Рыбкин В.В., Иванов А.Н., Смирнова К.В.** // *Химия Высоких Энергий.* 2017. Т. 51. N 1. С. 65-69. DOI: 10.1134/S0018143917010118.

Поступила в редакцию 10.03.2023
Принята к опубликованию 20.03.2023

Received 10.03.2023
Accepted 20.03.2023